Research Article

A Comparison Study of Some Metaheuristic Methods for Field Oriented Control Based Induction Motors

Hersh Hasan Taha Al-Dawoodi and Hilmi Aygun

Abstract—**Thanks to the accuracy, high reliability and excellent performance, field-oriented control (FOC) based induction motor (IM) drives are used in power applications. Generally, three PI controllers are used for speed control, and decoupling control of torque and flux provided by control of d-q components of stator current in FOC based IM. The common practice for tuning PI controller gains involves trial and error or the Ziegler-Nichols method. Unfortunately, these methods tend to lack effectiveness in achieving a robust dynamic response. In this paper, to overcome the drawbacks of classical PI tuning methods, some metaheuristic methods such as Grey Wolf Optimization (GWO), Artificial Bee Colony (ABC) and Particle Swarm Optimization (PSO) algorithms are used to determine the optimal values of the PI controller parameters to improve the dynamic performance of FOC based IM. A multi-objective function based on sum of absolute errors (SAE) is selected for this purpose. A detail comparison of methods is given in terms of convergence factor and control performance considering the transient response parameters. Control performance is evaluated under 3 operating conditions (constant reference speed at no load condition, variable reference speed at nominal load operation, and sudden load change condition). The simulation results indicate that, despite its slower convergence speed compared to other algorithms, the GWO algorithm achieves the best dynamic performance.**

Index Terms—**ABC, Field Oriented Control, GWO, Induction Motor, Metaheuristic, PSO.**

I. Introduction

Induction motors (IMs) are widely utilized across various applications, including household appliances, industrial facilities, automation systems, and even electric vehicles, owing to their straightforward design, cost-effectiveness, minimal maintenance requirements, high power density, and resilience in challenging environments [1]. Fig. 1 illustrates the cross-sectional structure of a squirrel cage IM. Stator windings are supplied with three-phase AC voltages, generating three-phase currents that produce a rotating magnetic field. This field induces a magnetic field in the rotor due to the short-circuited rotor bars. Consequently, a slip occurs between the speed of the rotating magnetic field, known as synchronous speed, and the rotor speed. The synchronous speed, as defined in Eq. (1), depends on the stator frequency and the number of poles. Therefore, the speed of an IM can be controlled by adjusting the stator frequency.

$$N_s = \frac{120f}{P} \tag{1}$$

Where N_s is the synchronous speed, f is the stator frequency and P is the pole number.

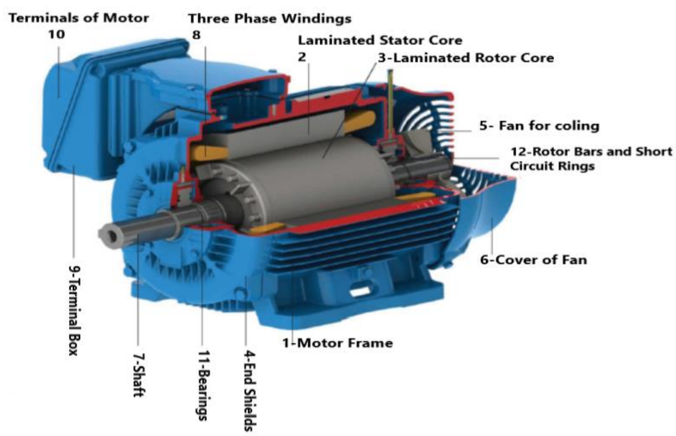

Fig. 1. Cross sectional structure of squirrel cage IM

Fast and precise torque response with effective flux regulation is a critical requirement for high-performance applications like robotics, rolling mills, and electric vehicles. Several methods such as field-oriented control (FOC), direct torque control (DTC) and space vector modulated direct torque control (DTC-SVM) have been proposed to obtain these requirements [2, 22-24]. This paper focuses on the FOC of IM drives.

HERSH HASAN TAHA AL-DAWOODI, is with Department of Electrical-Electronics Engineering University of Karabuk, Karabuk, Turkey, (e-mail: herieshhassan@gmail.com).

https://orcid.org/0009-0002-4158-7226

HILMI AYGUN, is with Department of Mechatronics Engineering University of Karabuk, Karabuk, Turkey, (e-mail: hilmiaygun@karabuk.edu.tr).

https://orcid.org/0000-0002-9073-2322

Manuscript received Aug 20, 2023; accepted Feb 22, 2024.
DOI: 10.17694/bajece.1346432

In FOC based drives, the decoupling control of torque and flux provides a high dynamic response. It is realized by control of *d-q* components of stator current individually. Generally, FOC method consists of three PI controllers used for speed control and *d-q* components control of stator current. The tuning of PI controller parameters presents a challenging problem, commonly addressed through trial and error or the Ziegler-Nichols method based on step response characteristics. Regrettably, these methods frequently lead to a diminished dynamic response, particularly in scenarios involving variable speed references and sudden load changes. In the literature, some controllers such as neuro-fuzzy controller [25], neural network controller [26], fuzzy logic controller [27], fuzzy logic-based PI controller [28], sliding mode controller [29] and backstepping controller [30] have been used for FOC of IM instead of conventional PI controllers. In contemporary research, there is a growing trend of employing metaheuristic optimization algorithms as alternative tools for optimizing PI controller parameters. This shift is driven by the need to overcome the drawbacks of traditional PI controllers.

In [3], Particle Swarm Optimization (PSO) was used to determine the optimal parameters of PI and PID controllers for the speed control. The findings indicate that PSO proved to be more effective in enhancing speed response and delivering greater stability compared to the Ziegler-Nichols method. In [4], Ant Colony Optimization (ACO) algorithm was used to tune online identification of the controller parameters in the vector control of IM during operation such as changes in mechanical and electrical parameters of IM. It improved the steady state characteristics and dynamic performance. In [5], a vector-control based IM drive was designed to improve efficiency and to decrease torque fluctuations. The PSO algorithm was employed to optimize the parameters of the PI controller. The outcomes demonstrated a notable reduction in torque fluctuations when these fluctuations were taken into account as part of the objective function. In [18], a self-tuned PID speed controller was designed by Artificial Bee Colony (ABC) algorithm to improve the robustness. In [19], indirect vector control of IM was realized by a Genetic Algorithm (GA) based PI controller. The speed response with the proposed controller was better than that with PI and PI-Fuzzy Hybrid controller in terms of settling time, rising time and overshoot.

In [6], the quantum-behaved lightning search algorithm (QLSA) was utilized to develop an optimal fuzzy speed controller and optimal PI current controllers. The results demonstrated that QLSA outperformed the lightning search algorithm (LSA), backtracking search algorithm (BSA), gravitational search algorithm (GSA), and PSO in terms of damping capability and enhancing transient responses during sudden changes in speed and load torque. In [7], a combination of Kharitonov's theorem and PSO was applied to design the PI controllers against parameters uncertainty.

In [8], a comparison study using PSO, JAYA algorithm and Teacher Learner based Optimization (TLBO) algorithm was presented for optimizing the parameters of Fractional-order PI (FOPI) and PI controllers. The results showed that JAYA algorithm provided a better response in steady state than the other algorithms.

Nomenclature

i_a , i_b , i_c	three-phase stator currents, A
i_d , i_q	two-phase stator currents, A
i_α , i_β	stator current components along α and β axes, A
V_d , V_q	two-phase stator voltages, V
V_α , V_β	stator voltage components along α and β axes, V
Ψ_d , Ψ_q	two-phase stator fluxes, Wb
R_s , R_r	stator and rotor resistances, Ω
L_s , L_r	stator and rotor inductances, H
L_m	mutual inductance, H
n_p	number of pole pair
J	inertia torque, kg m^2
f_d	friction coefficient, Nm s/rad
T_e	electromagnetic torque, Nm
K_t	torque constant
ω_s , ω_r	stator and rotor angular speeds, rad/s
ω_{sl}	slip angular speed, rad/s
τ_r	rotor time constant

In [9], population extremal optimization (PEO) algorithm was used to tune PID controller of speed control loop which had a two-degree-of-freedom (2-DOF) structure to provide smoother torque response.

In [20], PSO and GA algorithms based Parallel Proportional Integral (PPI) controllers were used to control the speed of FOC based IM. PSO based PPI controller exhibited a better dynamic response at high speeds. However, at low speeds, GA based PPI controller exhibited better results. In [21], the PI controllers were optimized by Grey Wolf Optimization (GWO) and TLBO. For the evaluation, several objective functions such as the integral time-multiplied absolute error (ITAE), Zwe-Lee Gaing's parameter (ZLG) and Mean Squared Error (MSE) were used. The best performance was obtained by GWO algorithm using ZLG objective function. Developed optimization algorithms for FOC based IM are listed in Table 1.

In this study, some metaheuristic methods such as GWO, ABC and PSO algorithms were used to obtain the optimal PI controller parameters not only for speed control loop but also for *d-q* component control loops of stator current to improve the dynamic performance of FOC based IM and the results were compared.

TABLE I
METAHEURISTIC ALGORITHMS FOR FOC BASED IM IN LITERATURE

Algorithm	**Optimization**	**Performance**
PSO [3]	Optimization of PI/PID speed controller	improved speed response and more stable results than Ziegler-Nichols method
ACO [4]	Optimization of PID speed controller	Improved dynamic performance and steady state characteristics
PSO [5]	Optimization of PI speed controller and flux controllers	Reduced torque fluctuations
QLSA [6]	Optimization of fuzzy speed controller and PI current controllers	Better performance in terms of damping capability, robustness, and improvement in transient responses than LSA, BSA, GSA and PSO
Combination of PSO and Kharitonov's theorem [7]	Optimization of PI speed controller and PI current controllers	A high level of stability against parameter uncertainty
Comparison of PSO, TLBO and JAYA [8]	Optimization of PI/FOPI speed controller and PI/FOPI current controllers	Better response in steady state by JAYA than other algorithms
PEO [9]	Optimization of 2-DOF PID speed controller	Superior performances of the 2-DOF control over the 1-DOF one in terms of torque smoothing and speed tracking
ABC [18]	Optimization of PID speed controller	Excellent dynamic response and robustness with self-tuned parameters
GA [19]	Optimization of PID speed controller	Better performance than PI and PI-Fuzzy Hybrid Controllers in terms of settling time, rising time and peak overshoot
Comparison of PSO and GA [20]	Optimization of PPI speed controller	At high speeds, better dynamic response with PPI-PSO. At low speeds, better dynamic response with PPI-GA.
Comparison of GWO and TLBO [21]	Optimization of PI speed controller and PI current controllers	Best performance by GWO using ZLG objective function

II. FIELD ORIENTED CONTROL METHOD

In the field-oriented control (FOC) of induction motor, a decoupling control of flux and torque provided by *d-q* components control of stator current is applied to obtain high dynamic performance. The operations are realized through the *d-q* rotating frame with the rotor flux vector. The field flux linkage component is aligned with the *d*-axis, and the torque component is aligned with the *q*-axis [10]. The electromagnetic torque can be expressed by Eq. (2).

$$T_e = \frac{3}{2} n_p \frac{L_m}{L_r} \left(\Psi_d i_q - \Psi_q i_d \right) \tag{2}$$

Where n_p is the number of pole pair, L_m is the mutual inductance, L_r is the rotor inductance, Ψ_d and Ψ_q are the *d-q* components of rotor flux, i_d and i_q are the *d-q* components of stator current. In the FOC method, *d*-axis of the reference frame is locked onto the rotor flux vector, so Ψ_q=0. Therefore, the torque equation given in Eq. (3) becomes like that of DC motors.

$$T_e = \frac{3}{2} n_p \frac{L_m}{L_r} \Psi_d i_q \tag{3}$$

Fig. 2 shows the general block diagram of FOC based IM. To control the speed, PI speed controller determines torque reference value (T_e^*) by using the speed error as the input. If the torque constant value (K_t) is defined as shown in Eq. (4) by utilizing from Eq. (3), the reference value of *q*-component of stator current (i_q^*) is obtained as shown in Eq. (5). Here, Ψ_d^* is the reference value of rotor flux which is determined by the user.

$$K_t = \frac{3}{2} n_p \frac{L_m}{L_r} \Psi_d^* \tag{4}$$

$$i_q^* = T_e^* / K_t \tag{5}$$

Also, the reference value of *d*-component of stator current is determined as shown in Eq. (6).

$$i_d^* = \Psi_d^* / L_m \tag{6}$$

To control the reference values of *d-q* components of stator current, two PI current controllers determine the reference values of *d-q* components of stator voltage (V_d^* and V_q^*). After the V_d^* and V_q^* are converted to the reference values of *α-β* components of stator voltage (V_α^* and V_β^*) by inverse park transformation, space vector pulse width modulation (SVPWM) is applied to the voltage source inverter (VSI) [11].

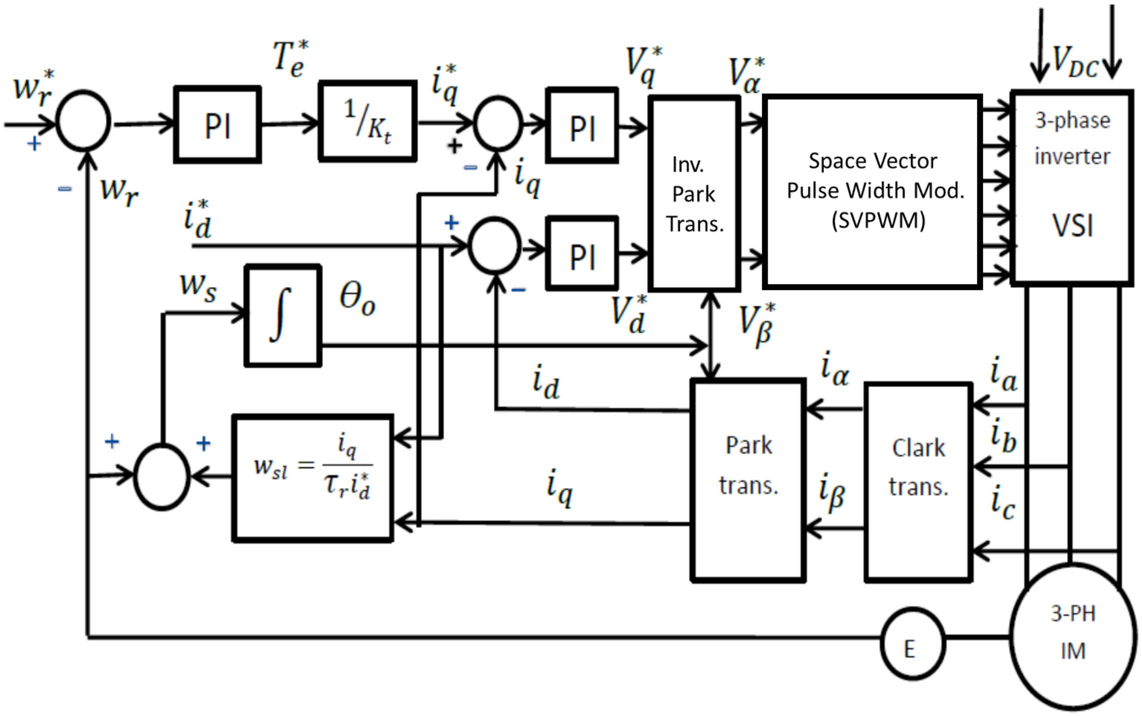

Fig. 2. Block Diagram of FOC based IM

III. METAHEURISTIC OPTIMIZATION METHODS

A. Grey Wolf Optimization Algorithm

In recent years, Grey Wolf Optimization (GWO) algorithm has been widely used in the optimization problems. This algorithm simulates the hunting behavior observed in grey wolves in their natural environment. The hierarchical structure consists of four distinct types of grey wolves: alpha, beta, delta, and omega, as illustrated in Fig. 3. The alpha wolves hold key responsibilities, including decisions related to hunting strategies, selection of sleeping locations, wake-up times, and other critical matters. Despite not being the physically strongest members, alphas excel in managerial abilities. The beta wolves play a supportive role by assisting the alphas in decision-making processes and contributing to various group activities. The lowest level in the hierarchy of the grey wolves is omega. In case of losing the omega, the group can have problems such as internal fighting. The rest of the grey wolves are called deltas. They have to submit to alphas and betas, but they dominate the omegas [12].

The main phases of hunting are shown in Fig. 3. The first one is approaching the prey. The second one is pursuing, harassing, and encircling the prey until the prey stops moving. The last one is attacking towards the prey. The encircling prey behaviour of grey wolves is mathematically modelled by the following equations.

$$\vec{D} = \left| \vec{C} \cdot \vec{X}_p(t) - \vec{X}(t) \right| \tag{7}$$

$$\vec{X}(t+1) = \vec{X}_p(t) - \vec{A} \cdot \vec{D} \tag{8}$$

Where t is the current iteration, $\vec{X}_p$ is the position vector of the prey, $\vec{X}$ is the position vector of any grey wolf. $\vec{A}$ and $\vec{C}$ coefficient vectors are given by the following equations.

$$\vec{A} = 2\vec{a} \cdot \vec{r}_1 - \vec{a} \tag{9}$$

$$\vec{C} = 2 \cdot \vec{r}_2 \tag{10}$$

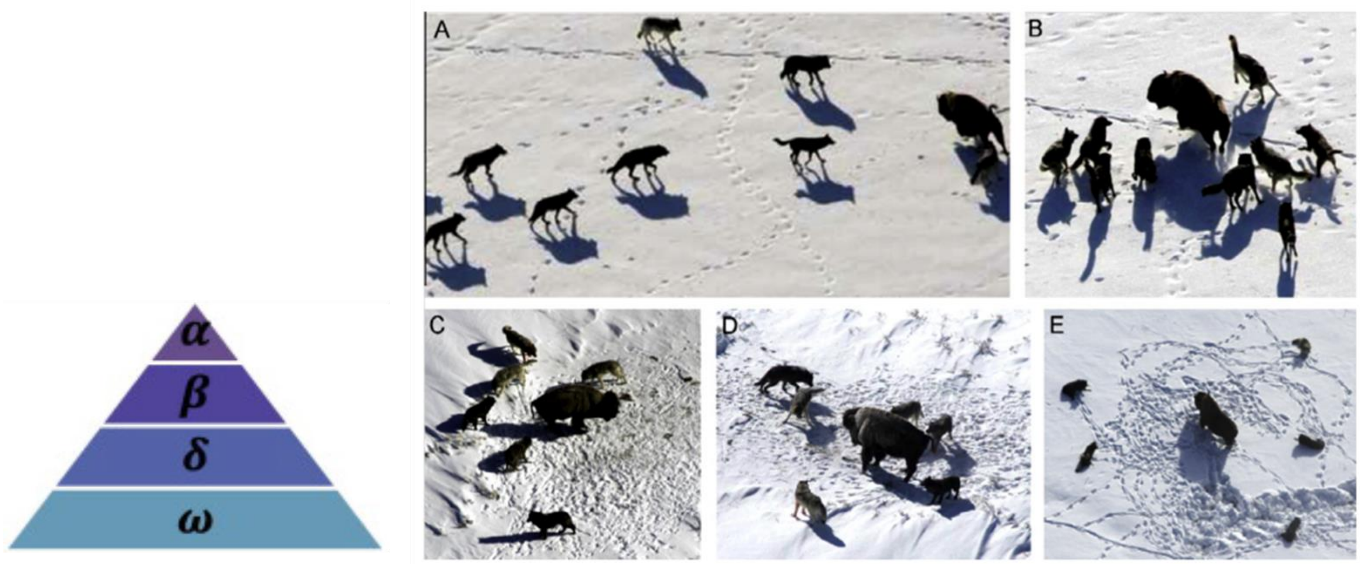

Fig. 3. Hierarchy and Hunting Behaviour of Grey Wolves: (A) Approaching the Prey (B-D) Pursuing, Harassing, and Encircling (E) Attacking [14]

Where $\vec{a}$ is reduced linearly from 2 to 0 during the iterations to model approaching the prey, $\vec{r}_1$ and $\vec{r}_2$ have random values in [0,1] range. To model the hunting behaviour of the grey wolves, the best three solutions are designated as alpha (α), beta (β), and delta (δ), respectively in every iteration, and they are used to update the positions of the other wolves including the omega (ω) by the following equations.

$$\vec{D}_{\alpha} = \left|\vec{C}_1 \cdot \vec{X}_{\alpha} - \vec{X}\right| \tag{11}$$

$$\vec{D}_{\beta} = \left|\vec{C}_2 \cdot \vec{X}_{\beta} - \vec{X}\right| \tag{12}$$

$$\vec{D}_{\delta} = \left|\vec{C}_3 \cdot \vec{X}_{\delta} - \vec{X}\right| \tag{13}$$

$$\vec{X}_1 = \vec{X}_{\alpha} - \vec{A}_1 \cdot \vec{D}_{\alpha} \tag{14}$$

$$\vec{X}_2 = \vec{X}_{\beta} - \vec{A}_2 \cdot \vec{D}_{\beta} \tag{15}$$

$$\vec{X}_3 = \vec{X}_{\delta} - \vec{A}_3 \cdot \vec{D}_{\delta} \tag{16}$$

$$\vec{X}(t+1) = \left(\vec{X}_1 + \vec{X}_2 + \vec{X}_3\right)/3 \tag{17}$$

Attacking the prey behaviour of the grey wolves depends on the $\vec{A}$ value. If $|\vec{A}| < 1$, it means that the wolves must attack the prey. Otherwise, if $|\vec{A}| > 1$, it means that the wolves must search a fitter prey. The flowchart depicting the GWO algorithm is illustrated in Fig. 4 [13].

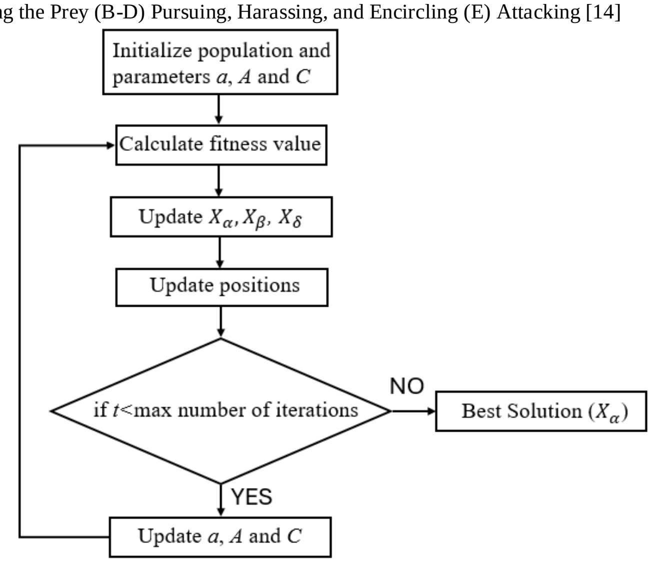

Fig. 4. The Flowchart of GWO Algorithm

B. *Artificial Bee Colony Algorithm*

Artificial Bee Colony (ABC) algorithm is an effective method for optimization problems. It models the foraging behavior of honeybees mathematically. There are three kinds of bees in the colony which are scout bees, employed bees, and onlooker bees. Scout bees search for undiscovered food sources by scanning the environment randomly. Employed bees exploit discovered food sources and share their position with onlooker bees. Onlooker bees go to the food sources for evaluating the quality of food [14].

In the ABC algorithm, the position of each food source corresponds to a potential solution of any optimization problem. The initial population is determined randomly in the search space. A selection process of food source is performed by onlooker bees by using the probability value given by Eq. (18) which depends on the fitness value of potential solutions.

$$p_i = \frac{fit_i}{\sum_{n=1}^{SN} fit_n} \tag{18}$$

Where fit_i is the fitness value of solution i, SN is the number of food sources. The fitness value corresponds to the quality of food source. To produce new solutions v_i in the neighborhood of x_i, the ABC uses the Eq. (19).

$$v_{ij} = x_{ij} + \phi_{ij}\left(x_{ij} - x_{kj}\right) \tag{19}$$

Where $k \in \{1, 2,\dots, SN\}$ and $j \in \{1, 2,\dots, D\}$ are the indexes. D indicates the dimensional size of the problem. Although k is selected randomly, it cannot be equal to i. ϕ_{ij} is a randomly determined number in the range of [-1,1]. In this algorithm, if a position cannot be improved during a predetermined number of cycles, the employed bee abandons that food source and the scout bee discovers a new food source to replace with the abandoned one. The discovered new food sources are determined in the search space randomly. The flowchart depicting the ABC algorithm is shown in Fig. 5 [15].

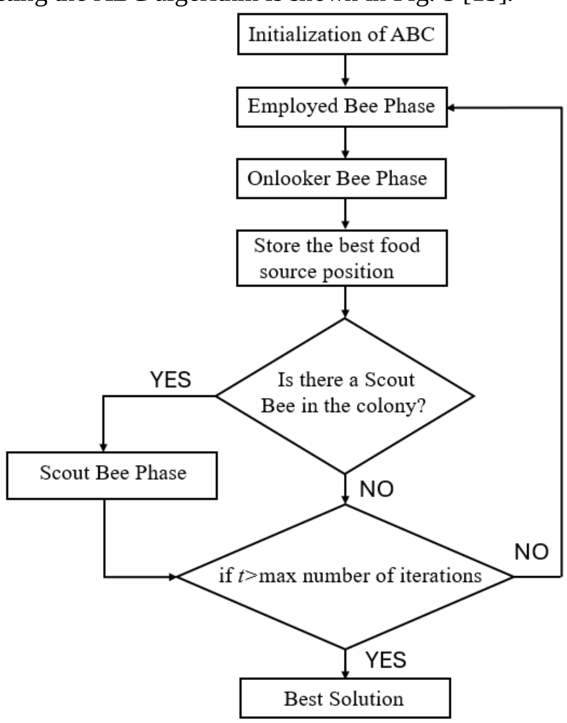

Fig. 5. The Flowchart of ABC Algorithm

C. Particle Swarm Optimization Algorithm

The Particle Swarm Optimization (PSO) algorithm stands as one of the most widely employed methods for optimization problems. Renowned for its ease of implementation, explorative capabilities, global convergence prowess, and robustness, PSO offers several advantages in tackling diverse optimization challenges. It models the behavior of birds to search the food [16].

In this algorithm the birds called particles have a position and a velocity. In every iteration, the fitness values of the particles are calculated due to the objective function. The best position of each particle is called the local best position of associated particle. The best position between the positions of all particles is called the global best position. The new velocity and position of each particle are calculated using the following equations, incorporating both the local and global best positions:

$$v_i(t+1) = \omega v_i(t) + c_1 r_1 (p_i(t) - x_i(t)) + c_2 r_2 (g(t) - x_i(t)) \tag{20}$$

$$x_i(t+1) = x_i(t) + v_i(t+1) \tag{21}$$

Where t represents the current iteration, i denotes the current particle, x is the position of the particle, v is the velocity of the particle, r_1 and r_2 are random values in the range of [0, 1], c_1 and c_2 are the constants influencing the particle's attraction to local and global best positions, p is the local best position of associated particle, g denotes the global best position and ω is the inertial weight. The PSO algorithm's flowchart is illustrated in Fig. 6 [17].

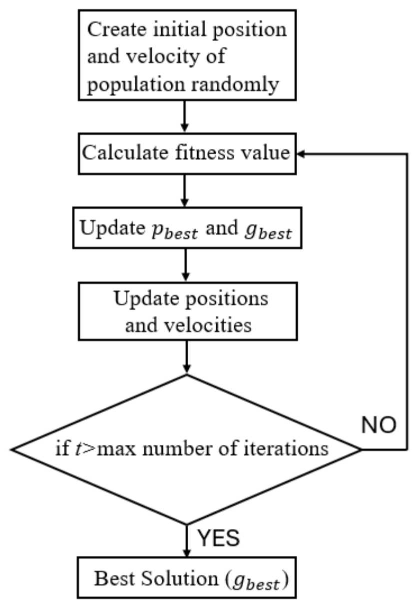

Fig. 6. The Flowchart of PSO Algorithm

IV. SIMULATION RESULTS

This paper employs metaheuristic algorithms such as PSO, GWO, and ABC to optimize the proportional and integral gains of PI controllers with the aim of enhancing the performance of FOC based IM. The model of the proposed method is illustrated in Fig. 7. Simulation results obtained using MATLAB are presented for three distinct operating conditions: no-load condition, speed change condition, and sudden load change condition. The parameters of the utilized induction motor are detailed in Table 2.

As the performance of FOC based IM is determined due to the three control loops (speed control loop and d-q component control loops of stator current), a multi-objective function is selected as given by Eq. (22) which consists of three terms based on Sum of Absolute Errors (SAE) index, being related to minimizing errors (e_ω, e_{isd} and e_{isq}) belong to mentioned control loops. SAE function for any variable is given by Eq. (23).

$$f_{\cos t} = \omega_1 SAE_\omega + \omega_2 SAE_{i_{sd}} + \omega_3 SAE_{i_{sq}} \quad (22)$$

$$SAE_x = \sum_{i=1}^{N} \left| x_r(i) - x_m(i) \right| \quad (23)$$

TABLE II
INDUCTION MOTOR PARAMETERS

Parameter	Value
Power	5.5 kW
Number of pole (P)	4
Stator resistance (R_s)	1.28333 Ω
Rotor resistance (R_r)	0.9233 Ω
Stator inductance (L_s)	0.141833 H
Rotor inductance (L_r)	0.143033 H
Mutual inductance (L_m)	0.137333 H
Inertia torque (J)	0.1 kg m^2
Friction coefficient (f_d)	0.0028 Nm s/rad

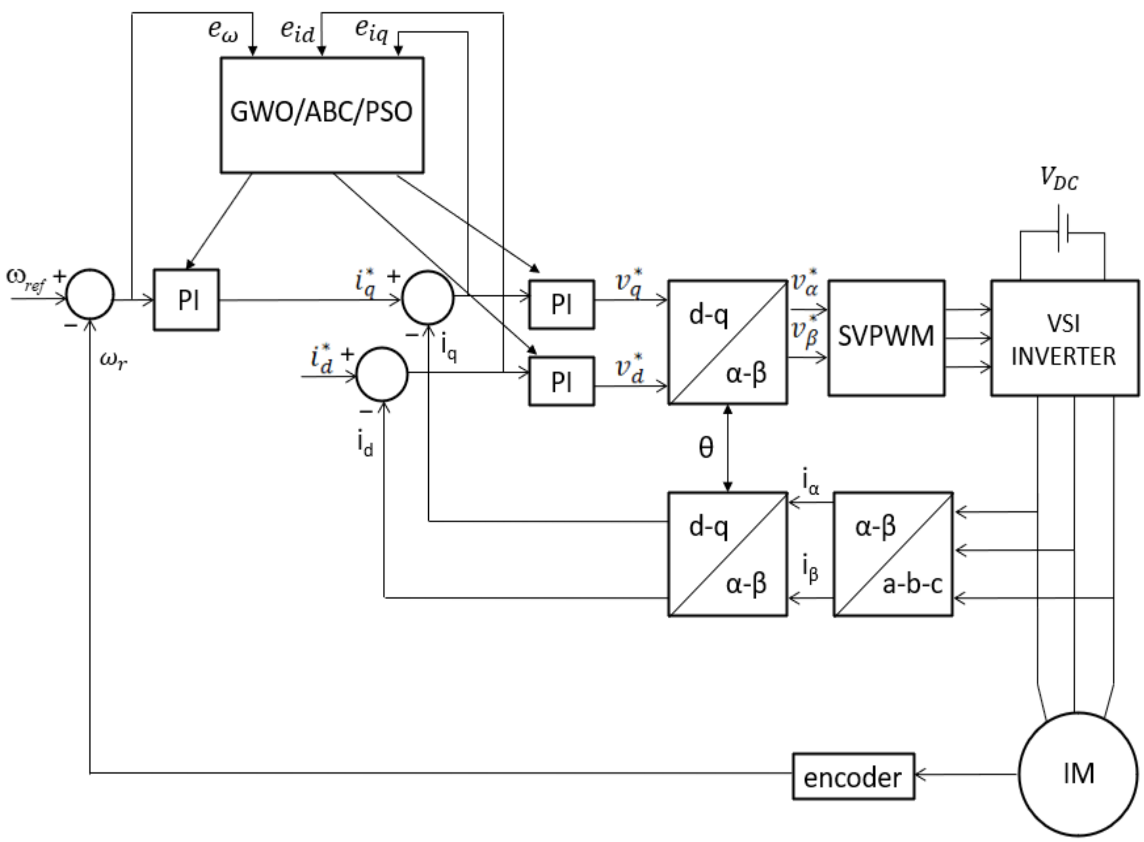

Fig. 7. Model of the Proposed Method

Where ω_1, ω_2 and ω_3 are weighting factors used to equalize the three terms in the same magnitude order, x_r and x_m show the reference and measured values respectively for x variable, and N is the element number of x variable.

The obtained PI controller gains by used metaheuristic algorithms are given in Table 3.

TABLE III
OPTIMIZED CONTROLLER GAINS

Controller	**K_p**			**K_i**		
	PSO	**ABC**	**GWO**	**PSO**	**ABC**	**GWO**
Speed Controller	5.76	6.36	6.60	500	500	500
i_{sq} controller	3.99	4.19	4.21	1700	1672.5	1663.9
i_{sd} controller	6.95	6.90	6.83	1170.13	1144.8	1163.2

In the initial phase, the FOC based IM was operated under no-load conditions with a reference speed of 75 rad/s. The speed responses generated by the metaheuristic algorithms are depicted in Fig. 8-a. Table 4 presents the performances of the utilized metaheuristic methods. The motor speed reaches the desired speed during no-load operation after approximately 0.183 seconds with the GWO and ABC methods, while the corresponding time with the PSO method is about 0.198 seconds. The settling time with GWO and ABC is 0.015 seconds shorter than that with PSO. Although the maximum overshoot (2.05%) is observed with PSO, the minimum overshoot (1.15%) is observed with GWO. However, the rise times of the methods are identical. Therefore, the performance of the speed controller based on GWO is superior. Additionally, it can be asserted that the ABC method outperforms the PSO method.

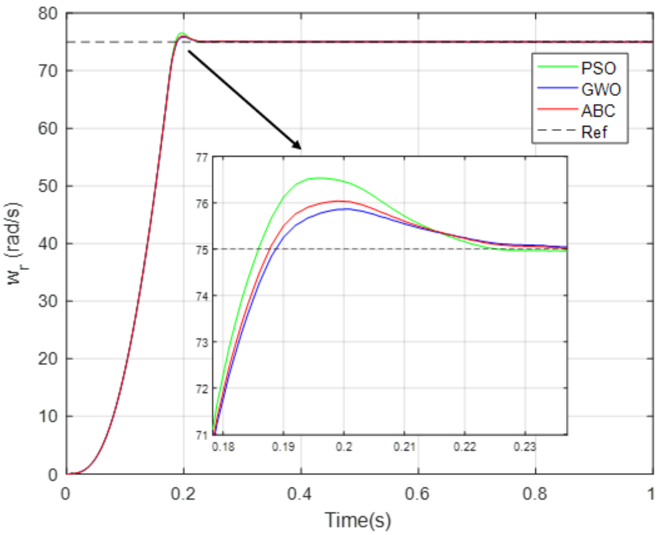

(a)

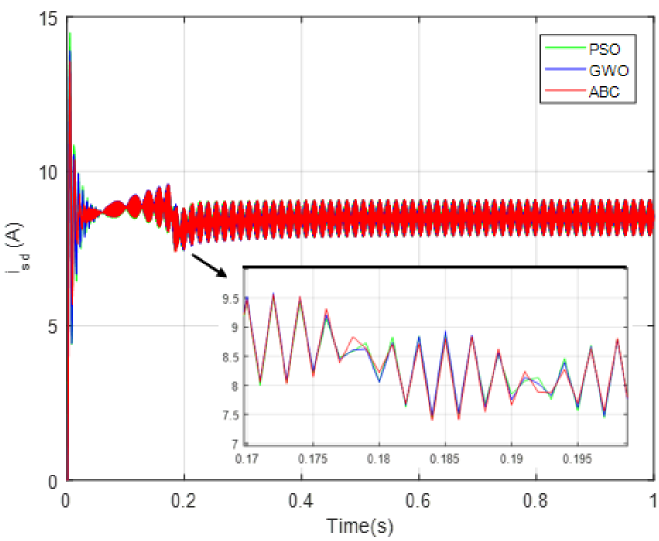

(b)

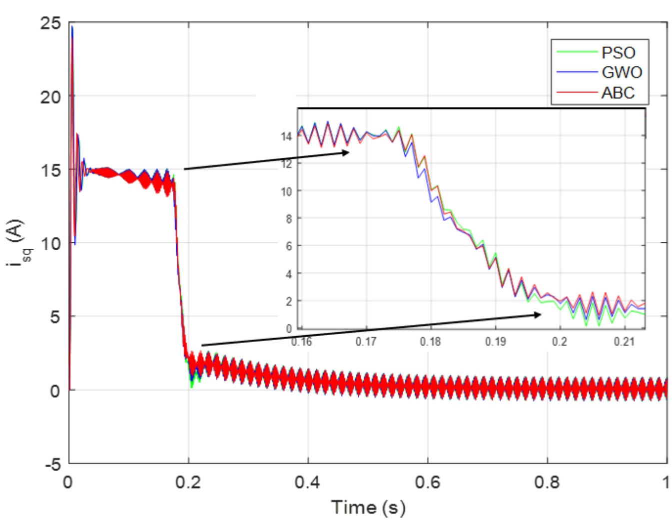

(c)

Fig. 8. No load condition test with a constant reference speed a) speed response b) i_{sd} current response c) i_{sq} current response

TABLE IV
COMPARISON OF METHODS AT NO LOAD CONDITION

Algorithm	**Rising time (s)**	**Settling time (s)**	**Maximum overshoot (%)**
PSO	0.1024	0.1988	2.05
GWO	0.1024	0.1838	1.15
ABC	0.1024	0.1833	1.39

Under identical conditions, the performance of the i_{sd} current controller is depicted in Fig. 8-b, while the performance of the i_{sq} current controller is illustrated in Fig. 8-c. It is observed that, for both current controllers, the outcomes of the three optimization methods do not exhibit significant differences.

Secondly, the performances of the methods are assessed under variable reference speed conditions at nominal load as depicted in Fig. 9. The reference speed is increased from 75 rad/sec to 150 rad/sec at the 1st second. Subsequently, at the 4th second, the reference speed is decreased from 150 rad/sec to -150 rad/sec to evaluate performance under reverse rotation conditions. Based on the speed response depicted in Fig. 9-a, it can be asserted that the control capability of the methods is effective under variable reference speed conditions, and the PI speed controller utilizing metaheuristic methods can effectively control the IM even when the rotation direction changes. This test comprises three transient cases, and in all instances, the GWO algorithm outperforms the other two methods. The minimum overshoot is 0.51% in the second transient case with GWO, while it is 0.64% in the third transient case using the same algorithm. On the other hand, the i_{sd} current response is depicted in Fig. 9-b. When the speed of the IM is increased from 75 rad/sec to 150 rad/sec, there is an increase in i_{sd} current ripple. According to the i_{sq} current response illustrated in Fig. 9-c, there is no significant difference among the three curves, even in transient conditions. As the speed of the IM increases, i_{sq} current ripple also increases.

Finally, a sudden load change test was conducted using the methods employed for FOC based IM. The load torque was increased from 0 Nm to 25 Nm in the 1st second and decreased from 25 Nm to 10 Nm in the 2nd second. Fig. 10-a illustrates the speed response of the IM. In the 1st second, the IM experiences a decrease in speed due to an increase in load torque, reaching the reference speed after a brief transient period. By the 2nd second, the IM speed increases due to a reduced load, stabilizing at the desired speed. Consequently, successful speed control is achieved by all methods. During sudden load changes, it is observed that the speed response is less influenced by the GWO and ABC algorithms. In the second transient case, following a load disturbance, the IM speed reaches the reference speed after 0.084 seconds and 0.088 seconds with ABC and GWO, respectively, while PSO achieves this in 0.074 seconds. In the third transient case, these times are 0.081 seconds, 0.085 seconds, and 0.074 seconds for ABC, GWO, and PSO, respectively. Hence, it can be asserted that the settling time in transient cases caused by load disturbances is minimized with PSO.

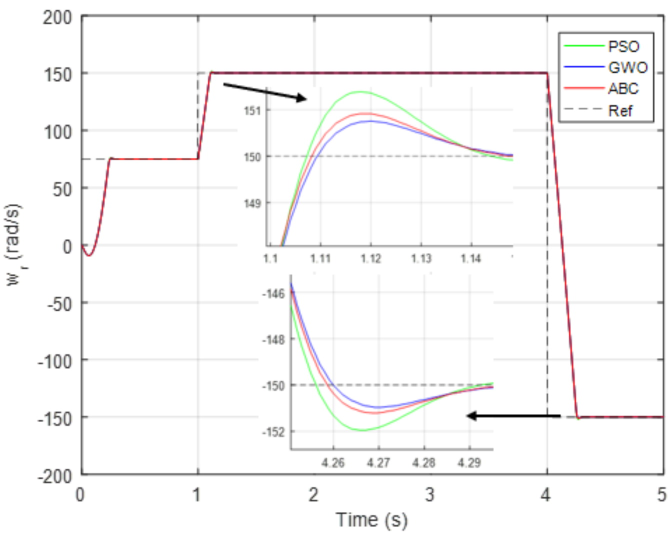

(a)

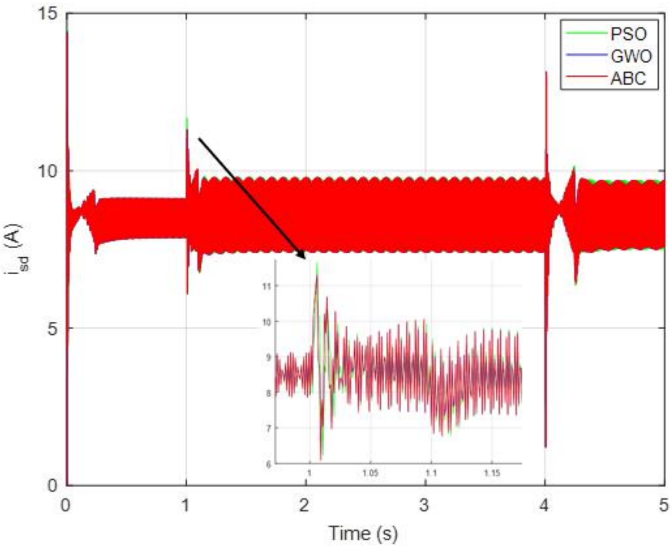

(b)

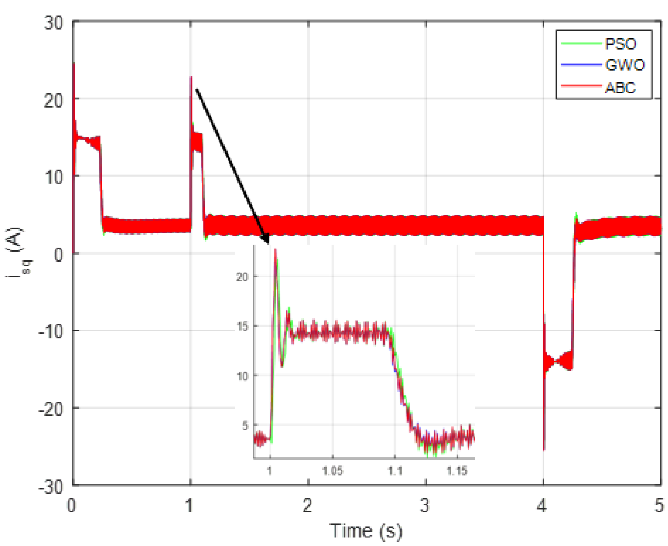

(c)

Fig. 9. Variable reference speed test under nominal operating condition
a) speed response b) i_{sd} current response c) i_{sq} current response

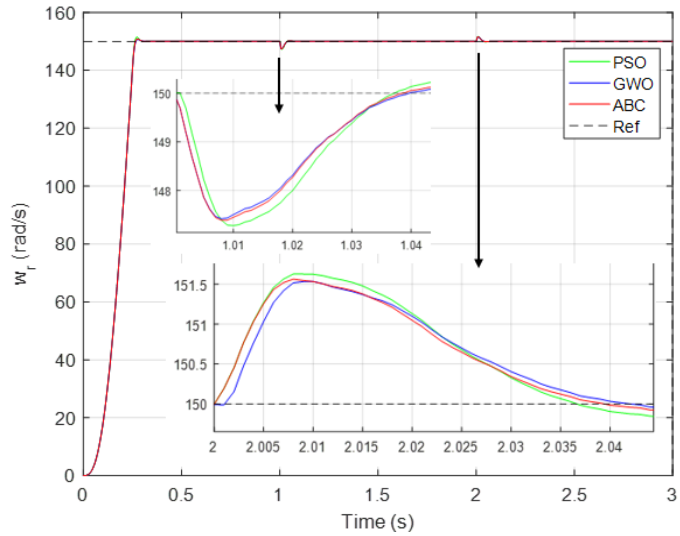

(a)

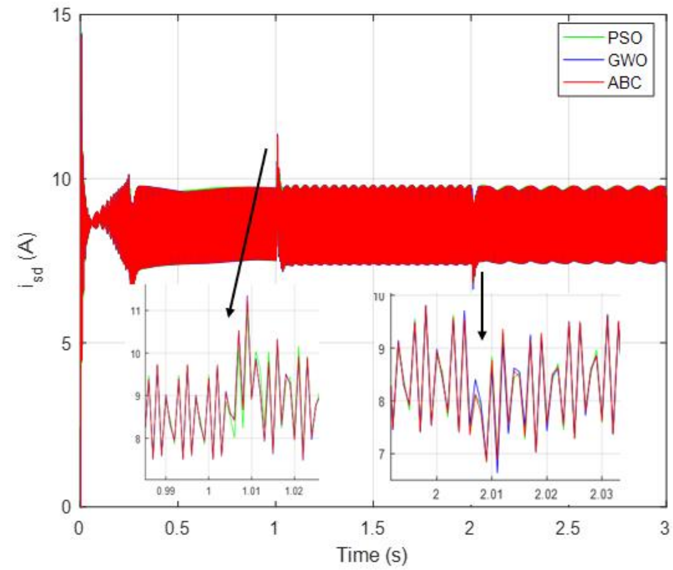

(b)

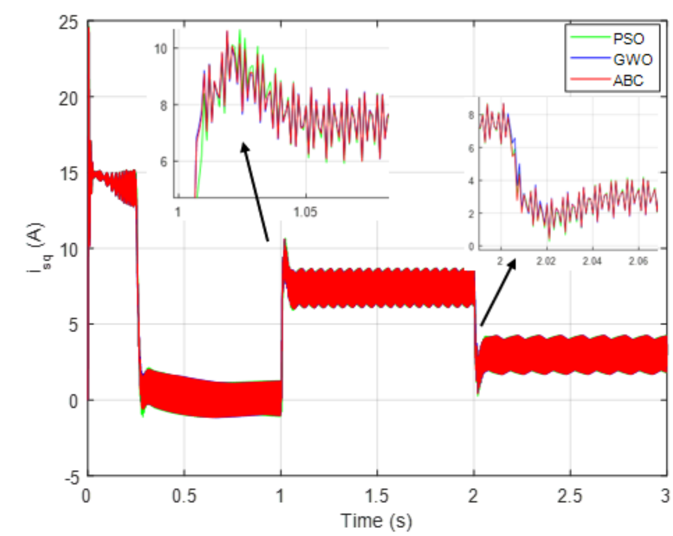

(c)

Fig. 10. Sudden load change test
a) speed response b) i_{sd} current response c) i_{sq} current response

The *d-q* current responses depicted by Figures 10-b and 10-c are nearly identical across all metaheuristic methods. Analyzing the steady-state values reveals that the i_{sd} current remains relatively stable, while the i_{sq} current undergoes significant changes. This is attributed to the impact of increased load torque on electromagnetic torque. In the FOC of the IM, the i_{sq} current governs the electromagnetic torque, leading to an increase in i_{sq} current with higher load torque, as illustrated in Fig. 10-c. Consequently, a decrease in load torque results in a lower i_{sq} current.

Fig. 11 illustrates the convergence speed of the applied metaheuristic algorithms. Notably, the ABC algorithm achieves optimal convergence by the 34th iteration, while the GWO algorithm converges by the 72nd iteration and PSO converges by the 41st iteration. Consequently, it can be concluded that the ABC algorithm exhibits the best convergence speed, with GWO being the least efficient in this regard.

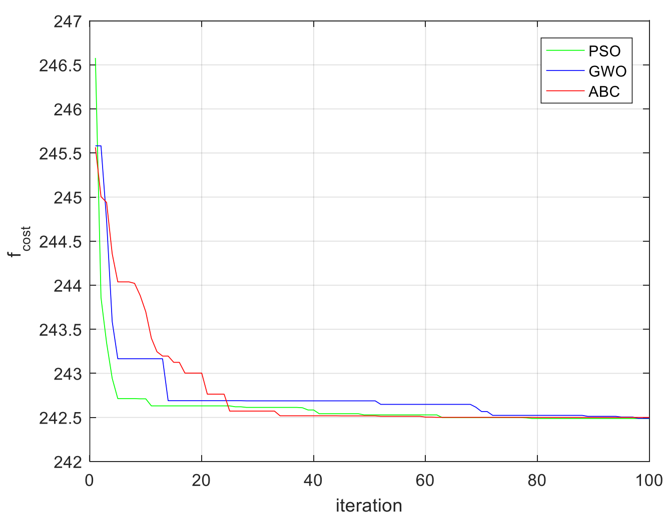

Fig. 11. Convergence speed of metaheuristic algorithms

Table 5 is given for a detail analysis of methods comparatively in terms of speed control performance by the transient response parameters and, convergence.

TABLE V
COMPARISON OF METHODS IN TERMS OF CONTROL PERFORMANCE AND CONVERGENCE

Condition	Parameters	PSO	GWO	ABC
Constant reference speed for no load operation	Rising time	same	same	Same
	Settling time	highest	same	Same
	Overshoot	highest	lowest	-
Variable reference speed for nominal load condition	Settling time	same	same	Same
	Overshoot	highest	lowest	-
Sudden load change test	Instant dropping in the speed	highest	same	Same
	Settling time	lowest	highest	-
Any condition	Convergence speed	-	slowest	Fastest

V. CONCLUSION

In this paper, the results of FOC based IM realized by optimization of PI controllers using the metaheuristic algorithms (PSO, GWO and ABC) are presented comparatively. The assessment is conducted based on the responses of the IM under three operational conditions: no-load, speed change at nominal load, and sudden load change. Under no-load and speed change conditions, the GWO algorithm yields the best dynamic performance, particularly in terms of maximum overshoot. Despite a change in the rotation direction during the speed change test, the control capability of the utilized controllers remains commendable. However, the *d-q* current responses are nearly identical across all methods. During load change conditions, the speed response is less impacted by the GWO and ABC algorithms due to load disturbances. Nevertheless, the settling time in transient cases is minimized with PSO. Consequently, the optimization of PI controllers in FOC-based IM is successfully accomplished through the application of metaheuristic methods. The findings indicate that the dynamic performance with the GWO algorithm surpasses that of PSO and ABC in FOC-based IM, although the convergence speed of the GWO algorithm to optimal results is slower compared to PSO and ABC algorithms.

ACKNOWLEDGEMENT

This paper was derived from the thesis called “Field oriented control of induction motor by metaheuristic methods” which is realized in Karabuk University in 2023.

REFERENCES

[1] I. Ferdiansyah, M.R. Rusli, B. Praharsena, H. Toar, E. Purwanto. "Speed control of three phase induction motor using indirect field oriented control based on real-time control system." 10th International Conference on Information Technology and Electrical Engineering (ICITEE), Bali, Indonesia, 2018.

[2] A.Y. Yousef, S.M. Abdelmaksoud. "Review on field oriented control of induction motor." International Journal for Research in Emerging Science and Technology, vol. 2. 7, 2015, pp 5–16.

[3] T. Banerjee, S. Choudhuri, J. Bera, A. Maity. "Off-line optimization of PI and PID controller for a vector controlled induction motor drive using PSO." 6th International Conference on Electrical and Computer Engineering (ICECE), Dhaka, Bangladesh, 2010.

[4] C. Lai, K. Peng, G. Cao. "Vector control of induction motor based on online identification and ant colony optimization." 2nd International Conference on Industrial and Information Systems, Dalian, China, 2010.

[5] M.B.B. Sharifian, S. Galvani, M.B. Kouhshahi. "Torque fluctuations reducing in a vector-controlled induction motor drive by PI controller tuning using particle swarm optimization.” International Conference on Electrical Machines and Systems, Beijing, China, 2011.

[6] M.A. Hannan, J.A. Ali, A. Mohamed, U.A.U. Amirulddin, N.M.L. Tan, M. N. Uddin. "Quantum-behaved lightning search algorithm to improve indirect field-oriented Fuzzy-PI control for IM drive." IEEE Industry Applications Society Annual Meeting, Cincinnati, OH, USA, 2017.

[7] F.A. Hasan, A.T. Humod, L.J. Rashad. "Robust decoupled controller of induction motor by combining PSO and Kharitonov’s theorem." Engineering Science and Technology, an International Journal, vol. 23. 6, 2020, pp 1415–1424.

[8] A. Raj, Y.A. Khan, V. Verma. "Comparative evaluation of PSO, TLBO, and JAYA based adaptive PI and FOPI controllers for vector controlled induction motor drive.” IEEE 4th International Conference

on Computing, Power and Communication Technologies (GUCON), Kuala Lumpur, Malaysia, 2021.

[9] M.M. Hasan, M.S. Hussain, M.S. Rana, M.H.K. Roni. "Population extremal optimization based 2-DOF control strategy for field oriented control of induction motor." 3rd International Conference on Electrical & Electronic Engineering (ICEEE), Rajshahi, Bangladesh, 2021.

[10] M.J. Cheerangal, A.K. Jain, A. Das. "Control of rotor field-oriented induction motor drive during input supply voltage sag." IEEE Journal of Emerging and Selected Topics in Power Electronics, vol. 9. 3, 2021, pp 2789-2796.

[11] R. Rai, S. Shukla, B. Singh. "Sensorless field oriented SMCC based integral sliding mode for solar PV based induction motor drive for water pumping." IEEE Transactions on Industry Applications, vol. 56. 5, 2020, pp 5056-5064.

[12] S. Mirjalili, S.M. Mirjalili, A. Lewis. "Grey wolf optimizer." Advances in Engineering Software, vol. 69, 2014, pp 46-61.

[13] M.A. Şen, M. Kalyoncu. "Optimal tuning of PID controller using grey wolf optimizer algorithm for quadruped robot." Balkan Journal of Electrical & Computer Engineering, vol. 6. 1, 2018, pp 29-35.

[14] D. Karaboga, B. Basturk. "On the performance of artificial bee colony (ABC) algorithm." Applied Soft Computing, vol. 8, 2008, pp 687-697.

[15] D. Karaboga, C. Ozturk. "A novel clustering approach: Artificial Bee Colony (ABC) algorithm." Applied Soft Computing, vol. 11, 2011, pp 652-657.

[16] J. Kennedy, R. Eberhart. "Particle swarm optimization." International Conference on Neural Networks, Perth, WA, Australia, 1995.

[17] A. Iqbal, G.K. Singh. "PSO based controlled six-phase grid connected induction generator for wind energy generation." CES Transactions on Electrical Machines and Systems, vol. 5. 1, 2021, pp 41-49.

[18] E. Ebrahim. "Artificial bee colony-based design of optimal on-line self-tuning PID-controller fed AC drives." International Journal of Engineering Research, vol. 3. 12, 2015, pp 807-811.

[19] S. R. Ahamed, J. N. Chandra Sekhar, D. P. Reddy P. "Speed control of induction motor by using intelligence techniques." International Journal of Engineering Research and Applications, vol. 5. 1, 2015, pp 130-135.

[20] T. G. Workineh, Y. B. Jember, A. T. Kassie. "Evaluation of intelligent PPI controller for the performance enhancement of speed control of induction motor." Scientific African, vol. 22, 2023, pp 1-16.

[21] P. J. Shaija, A. E. Daniel. "Optimal tuning of PI controllers for IM drive using GWO and TLBO algorithms." 5th International Conference on Electrical, Computer and Communication Technologies (ICECCT), Erode, India, 2023.

[22] B. Çavuş, M. Aktaş. "MPC-based flux weakening control for induction motor drive with DTC for electric vehicles." IEEE Transactions on Power Electronics, vol. 38. 4, 2023, pp 4430-4439.

[23] K. V, B. Singh. "Optimized reference points based vector control of induction motor drive for electric vehicle." IEEE Transactions on Industry Applications, vol. 59. 4, 2023, pp 4164-4174.

[24] A. Benhammou, H. Tedjini, Y. Guettaf, M. A. Soumeur, M. A. Hartani, O. Hafsi, A. Benabdelkader. "Exploitation of vehicle's kinetic energy in power management of tow -wheel drive electric vehicles based on ANFIS DTC-SVM comparative study." International Journal of Hydrogen Energy, vol. 46, 2021, pp 27758-2769.

[25] H. Sathishkumar, S. S. Parthasarathy. "A novel neuro-fuzzy controller for vector controlled induction motor drive." Energy Procedia, vol. 138, 2017, pp 698–703.

[26] H. Sathishkumar, S. S. Parthasarathy. " A novel neural network intelligent controller for vector controlled induction motor drive." Energy Procedia, vol. 138, 2017, pp 692–697.

[27] Z. Tir, O. P. Malik, A. M. Eltamaly. "Fuzzy logic based speed control of indirect field oriented controlled double star induction motors connected in parallel to a single six-phase inverter supply." Electric Power Systems Research, vol. 134, 2016, pp 126-133.

[28] S. Pravallika, J. N. Chandra sekhar, D. P. Reddy P. "Optimization of Speed Control of Induction Motor Using Self Tuned PI plus Fuzzy Hybrid Controller." International Journal of Emerging Technology and Advanced Engineering, vol. 5. 1, 2015, pp 258-262.

[29] S. P J, A. E. Daniel. "Robust sliding mode control strategy applied to IFOC induction motor drive." 4th International Conference on Electrical, Computer and Communication Technologies (ICECCT), Erode, India, 2021.

[30] A. Zaafouri, C. B. Regaya, H. B. Azza, A. Châari. "DSP-based adaptive backstepping using the tracking errors for high-performance sensorless speed control of induction motor drive." ISA Transactions, vol. 60, 2016, pp 333-347.

BIOGRAPHIES

HERSH HASAN TAHA AL-DAWOODI joined the College of Engineering, Department of Electrical at Tikrit University in 2008. He also received the M.S. degree in electrical and electronics engineering from Karabuk University, Karabuk, Turkey, in 2023. His research interests include control of synchronize generator, PV system control, power factor correction.

HILMI AYGUN received the B.S. degree in electrical and electronics engineering from Kirikkale University, Kirikkale, in 2007. He also received the M.S. and Ph.D. degrees in electrical and electronics engineering from Karabuk University, Karabuk, Turkey, in 2011 and 2019, respectively. From 2009 to 2019, he was a Research Assistant at Karabuk University. Since 2019, he has been an Assistant Professor with the Mechatronics Engineering Department, Karabuk University. His research interests include control of electrical machines, electric vehicles, optimization by metaheuristic algorithms.